The Pennsylvania State University

The Graduate School

Department or Graduate Program

INVESTIGATION OF 3D PRINTED POLYMER AND METAL SUBSTRATES FOR OPTICAL MIRRORS

A Thesis in

Electrical Engineering

By

Joshua C Davidson

Submitted in Partial Fulfillment

of the Requirements

for the Degree of

Master of Science

December 2019

The thesis of Joshua C Davidson was reviewed and approved* by the following:

Timothy Joseph Kane
Professor of Electrical Engineering
Thesis Advisor

Ram Mohan Narayanan
Professor of Electrical Engineering

Kultegin Aydin
Professor of Electrical Engineering
Head of the Department of Electrical Engineering

*Signatures are on file in the Graduate School

ABSTRACT

In this study, experiments are conducted to investigate the surfaces of additively manufactured polymer and metal substrates. Polymer substrates undergo a surface treatment methodology that includes resin dipping, metallizing, and electroplating. Whereas, metal substrates undergo electroplating directly without the need for preceding treatments. The flatness and curvature of the printed substrates is measured and compared to their 3D models. Surface quality and surface roughness are evaluated before and after electroplating to determine the feasibility of 3D printed optical mirrors. Integration and optimization of additive manufacturing techniques with surface treatment methodologies will enable the production of complex and geometrically unique optical designs beyond the capabilities of conventional manufacturing techniques.

Keywords: Additive Manufacturing, Electroplating, Optics, Mirrors, Freeform, Gradient Index, GRIN, Stereolithography, Laser Sintering, Powder Bed

TABLE OF CONTENTS

LIST OF FIGURES

LIST OF TABLES

ACKNOWLEDGEMENTS

We would like to thank Dr. Abdalla Nassar from the Applied Research Lab at The Pennsylvania State University for supporting some of this work. We also thank our colleagues, Andrew Fitzgerald for his expertise electroplating components and Dr. Bangzhi Liu for helping with FESEM imaging at the Nanofabrication Lab, Materials Research Institute.

Some of this work was supported by US Army Night Vision and Electronic Sensors Directorate (NVESD) Contract Number W909MY-12-D-0008 through MTEQ Purchase Order 27701. We appreciate technical discussions with Dr. Nibir Dhar of NVESD.

Chapter 1

Introduction

This investigation considers the feasibility of producing optical-quality mirrors using common additive manufacturing techniques. Selected coating procedures are used to account for imperfections during printing. Dimensional characteristics such as flatness and curvature as well as surface characteristics such as surface quality and surface roughness are used to determine the feasibility of the approach. While there are many additive manufacturing processes, polymer-based stereolithography (SLA) and metal-based powder bed fusion are the primary techniques discussed throughout this report.

The methodology section provides details on the printers and materials used for this report while considering alternative options. The methodology also includes coating procedures for surface enhancement after 3D printing. A brief comparison between additive manufacturing and conventional manufacturing is discussed.

Experimental results and observations are separated into two sections, polymer substrates and metal substrates, with several subsections. For polymer and metal substrates, a flat disc and a convex dome are used for comparison. The polymer section involves a more extensive investigation on the coating procedure such that a post-curing method is conducted to obtain a smoother surface. The metal section includes an additional sample piece that demonstrates surface roughness as a function of inclination angle and explores the diameter accuracies of various through-holes.

The discussion provides details on the novelty of this investigation and why it should be explored further. The conclusion is a summary of the report and includes relevant applications additive manufacturing would most certainly be advantageous for.

Chapter 2

Methodology

This section will discuss techniques for additive manufacturing polymers and metals. The coating procedure conducted for polymers and metals will be explained but further details will be referenced to previous work [1]. Measurement techniques to obtain qualitative and quantitative data used for this report are examined.

Additive Manufacturing

Conventional manufacturing capabilities employ a subtractive approach, or removing of material, such that the parts are machined, milled, or polished to obtain a final product. Additive manufacturing is a technology with the potential to replace conventional methods by employing an additive approach, or adding material, such that the parts are created layer by layer using various techniques discussed in the following sections. The next two chapters focus on the surface quality and surface roughness of 3D printed parts which typically depend on the printing process. For this report, these processes will be separated into two categories: polymer-based and metal-based.

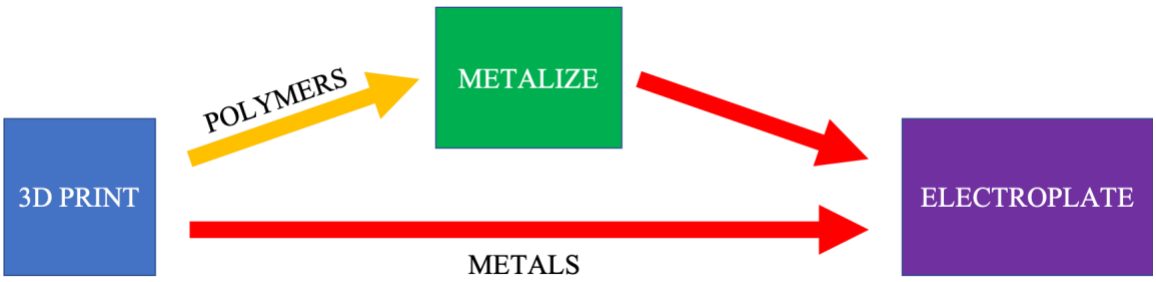

Figure **2-1**: Procedure for electroplating 3D printed polymers compared to metals.

Polymer-based

Common techniques for 3D printing polymers are selective laser sintering (SLS), fused deposition modeling (FDM), and stereolithography (SLA) [2,3]. SLS uses a laser to melt and bind powder particles while FDM uses a heated nozzle to extrude and bind thermoplastic filament. For this report, however, a Form 2 from Formlabs uses SLA to print polymer substrates. An ultraviolet laser with a 140μm spot size cures photopolymer resin along a path determined by the software into an isotropic, solid replica of the 3D model. A layer thickness between 20-50 μm is achievable which is responsible for the vertical resolution of sloped surfaces. Further information can be found in earlier work [1].

Metal-based

Common techniques for 3D printing metals are wire feed, powder bed fusion, and powder feed [4]. Similar to FDM, the wire feed technique uses an energy source to melt metal wire along a given path. Powder bed fusion systems rake powder particles across the build plate and use an energy source to melt or sinter the particles into a solid, 3D structure. Powder feed systems differ slightly from powder bed fusion because the powder particles are fed through the same nozzle used to emit the energy source. An energy source is typically a laser or electron beam. Both, wire feed and powder feed systems, are capable of large build volumes. Wire feed systems generally require more post-processing than the other techniques. Powder bed fusion systems are capable of printing high resolution parts and features such as internal cavities, but has a much smaller build volume. For this report, an EOS M280 Powder Bed Fusion system with a 90μm laser beam diameter and 40μm layer thickness is used to produce EOS Nickel Alloy Inconel 625 metal substrates. The system uses Argon as the process gas and has a powder sieving

module with a mesh size of 63 μm. Therefore, particles with a diameter greater than 63 μm will not be used during the printing process. Additionally, shot-peening and thermal post-processing are standard strategies used for metal additive manufacturing, but the experiments in this report do not explore either of the strategies. As an alternative, a single dome is bead-blasted, similar to shot-peening, and tested to observe differences. Also, the substrates were 3D printed on a thick metal plate to have greater control over thermal stresses. The parts were cut from the metal plate using electric discharge machining (EDM).

The bead-blasted dome is tested with Aluminum Oxide beads using #320 grit and #270-400 mesh size. The pressure is set to 50 PSI, aimed at a 45° incident angle about 3 inches from the substrate for 5 minutes. After bead-blasting, the substrate was sonicated in Acetone for 20 minutes.

Coating

The coating techniques relevant to this report are post-print resin dipping, electron beam physical vapor deposition (EBPVD), direct-current (DC) electroplating, and pulse-reverse-current (PRC) electroplating. While alternative options exist, the procedure executed throughout this report is subject to resource and equipment availability. The coating procedure for polymers differs from that of metals because a post-print resin dipping method and EBPVD is performed.

The post-print resin dipping method coats the 3D printed substrate with liquid resin, filling in grooves, and cures the liquid to form bonds with the imperfect surface. The result typically provides a smoother surface. Previous work explored this concept and proved its effectiveness [1].

EBPVD is implemented only for polymers because a metallic layer needs to be deposited to establish a conductive surface for electroplating. EBPVD is a useful coating technique that

enables the user to conformally deposit very fine grains for a variety of materials. Adhesion and material compatibility must be considered. For polymer-substrates, oxygen-plasma treatment is performed to enhance adhesion. Then, a thin bottom layer of Chrome and a thicker top layer of Nickel is deposited. These materials not only adhere well to one another - Chrome to plastic, Nickel to Chrome – but also possess similar thermal coefficients, an important factor to consider due to the high vacuum, high temperature environment.

Two electroplating techniques are performed for this report, DC and PRC. DC plating is used to forcefully deposit a thick layer of Nickel onto the surface in a short time to establish a greater and more uniform surface conductivity. About 1 μm can be deposited per minute. DC plating is used for select substrates requiring greater conductivity. The majority of the substrates are not DC plated. PRC plating is a process where the current is pulsed in the forward and reverse direction to trigger a fluctuation of laminating and delaminating of Nickel. A leveling agent is used to improve the process. In previous work, PRC plating demonstrates the ability to bridge small gaps, smooth rough surfaces, and reduce maximum peak size. The majority of the substrates are PRC plated.

Measurement

Scanning electron microscopy (SEM) and optical profilometry (OP) are the primary measurement techniques used throughout this report. SEM images provide information about surface quality characteristics such as grain size, cracks, pinholes, and other features. Not only can SEM image a larger area than OP, but it is generally a quicker process. However, SEM struggles to obtain 3-dimensional information. OP is capable of measuring the surface profile and surface roughness as well as calculating several parameters used for characterizing the surface.

For this report, a standard procedure is maintained for OP measurements. SEM imaging

is relatively straightforward; none of the SEM data contains stitched images. Whereas, nearly all the OP data contains stitched images. The measurement of dome substrates will be discussed; flat substrates have a similar procedure but is not as complicated. Since dome substrates have a curved profile, there are a few approaches to obtain data. The strategy for this report stitches several overlapping images, or patches, along the radial direction to obtain the curvature and the surface roughness in a single scan. The settings include: surface measure type, 3x CSI, high, subtract system reference, and extended scan. Each scan begins from the peak of the convex surface. It is a time-consuming process and has a few limitations that must be considered. To acquire the best image along the dome's curvature without changing the orientation, an objective lens with a magnification of 50x, numerical aperture of 0.55, and zoom of 0.5x is applied. This limits the measurement to a 3.4mm working distance and a patch size of about 300μm x 300μm. The tradeoff is better image quality for longer measurement time and smaller area under evaluation. For this report, high resolution imaging is prioritized. With this approach, a working distance of 3.4 mm along a sloped surface restricts the length the objective lens can travel radially from the peak on a convex surface and still remain in focus without crashing into the substrate. Hence, only a portion of the radius is measured from the peak. The scan length is set such that the maximum Z-height allows the peak of the surface to be in focus and the minimum Z-height allows the greatest radial length from the peak to be in focus, while remaining within the working distance. The optical profilometer must scan from the maximum to the minimum Z-height for each individual patch which causes this process to be very time-consuming.

There are other approaches that could be used but they are not feasible for this report. Several individual patches could be measured, selectively or randomly, along the slope to generate a compilation of data for given regions. Each patch could be a single image and the substrate could be oriented such that the area under examination is normal to the laser beam. This approach would likely be the quickest and provide an average for patches in the same region

along the slope. However, it is very difficult to measure the 300μm x 300μm patch a second time to compare before-and-after effects. In addition, the curvature cannot be measured using this approach. A different strategy could measure concentric rings which would obtain very accurate data as a function of the slope but would require an increasing number of stitched patches as the radius of the ring increases.

Chapter 3

Experimental Results and Observations for Polymer Substrates

Dimensional Characterization – Polymer Substrate

This section briefly discusses the flatness and the curvature of a printed polymer-substrate. Deviations from the CAD model are examined. Optical profilometry provides information about the flatness and the curvature. Data for testing the diameter accuracy is not available because data obtained from the ZEISS Smartzoom was difficult to extract and inconsistent throughout tests of the same substrate.

Flatness

Figure **3-1** shows cross-sectional images of a single substrate throughout the printing and coating procedures. The CAD model consists of a flat disc. After 3D printing, the substrate appears to have a sinusoidal surface. Other polymer-substrates have similar results. This is likely a consequence of the printing process. However, since each image is processed using a form remove of a plane, the sinusoid may also be an artifact from Mx software's data processing. After the high vacuum and high temperatures during EBPVD, the surface takes on a quadratic

appearance with a vertical variation of 50 µm along a horizontal segment of 10,000 µm. These results are not ideal and need to be accounted for by avoiding high vacuum, high temperature or by modifying the CAD model with an appropriate foundation. A thicker base or smaller diameter may reduce the sinusoidal appearance. Fixing the substrate to a larger base less prone to thermal stress may reduce the quadratic appearance.

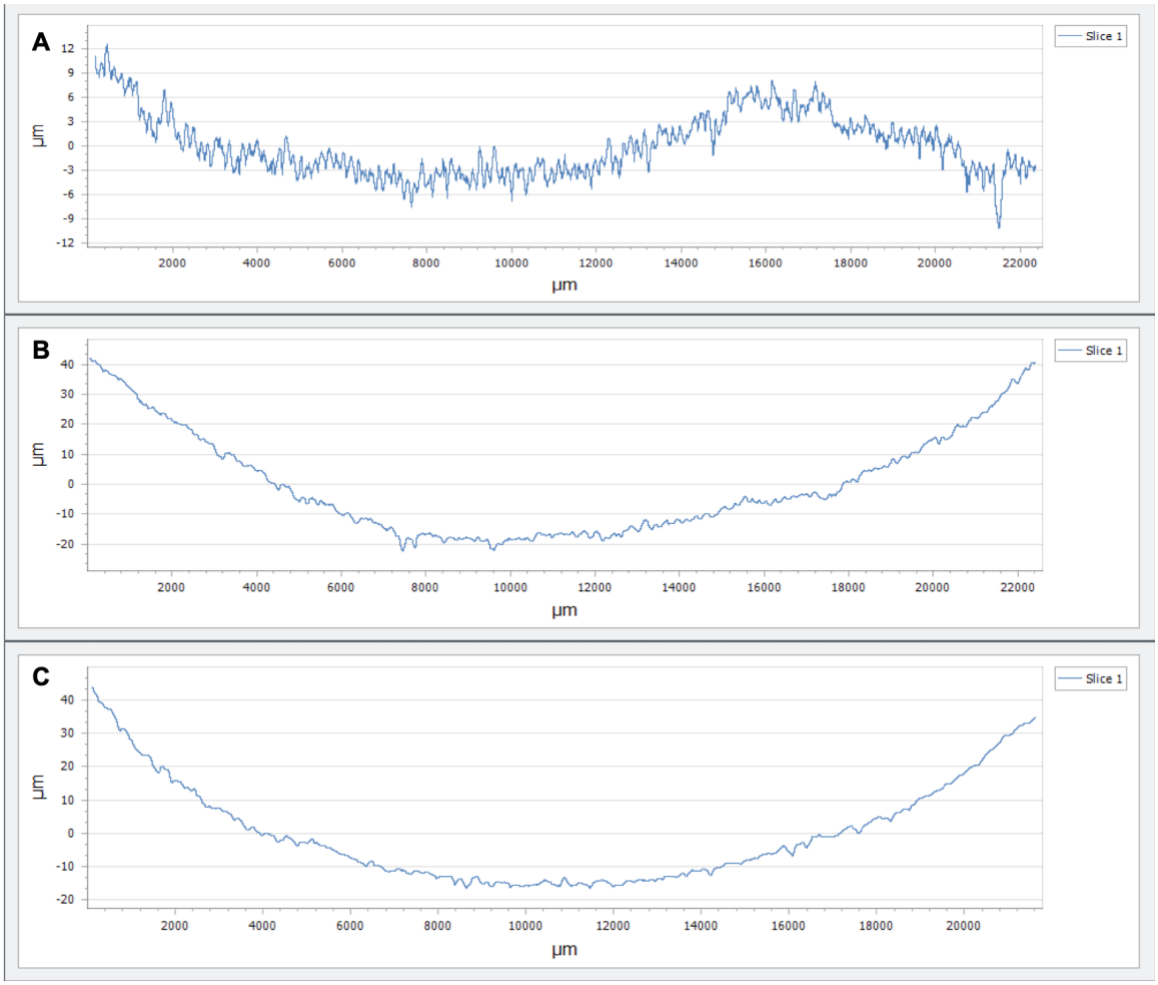

Figure **3-1**: Flatness data for polymer flat surface. Plane form remove. (A) Post-3D printed, (B) Post-EBPVD, (C) Post-PRC Plated.

Curvature

Figure **3-2** is a scatter plot of OP data points obtained from a cross section of a single polymer-substrate. The CAD model consists of a convex dome with a radius of curvature equal to 15 mm and a conic constant equal to -2. The CAD model is represented by the green reference line. Each curve is intentionally shifted along the vertical axis to be incident at the same point. No form remove is used in the Mx software. The radius of curvature is typically used for spherical lenses to identify the size of sphere that would create the desired curvature. For a flat optic, the radius would approach infinite. Assuming the data in Figure **3-2** is an accurate depiction of the true curvature, the results show a gradual increase in the radius of curvature from the 3D printed substrate. The 3D printed dome and post-EBPVD dome demonstrate a similar radius of curvature as the CAD model. After plating, however, the dome appears to have the greatest change.

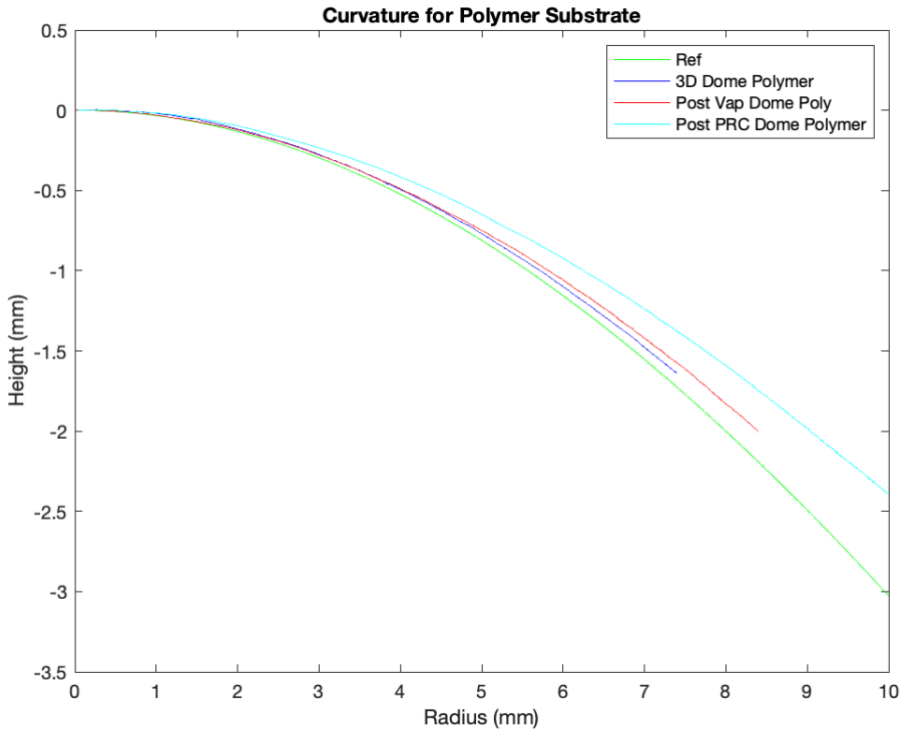

Figure **3-2**: Polymer dome curvature plot.

Surface Characterization – Polymer Substrate

This section provides a review of the surface quality and the surface roughness using information obtained from OP data and SEM images. Earlier work will be included and referenced. The section on surface quality discusses grain sizes and imperfections such as cracks and pinholes. The section on surface roughness discusses how the roughness varies after each coating procedure using a before-and-after approach.

Surface Quality

SEM images are provided to characterize grain sizes and imperfections on the surfaces of polymer-substrates.

Grain Size

The surface of a 3D printed polymer dome is presented in Figure **3-3**. The periodic lines produced by the laser swath are evident in Figure **3-3A**. Although the layer resolution of the SLA printer is 20-50 μm, the surface appears rocky and not very smooth in Figure **3-3B**. This is an example of a substrate without resin dipping after 3D printing. Previous work shows the outcome of resin dipping which is also referred to as post-curing. After EBPVD, surfaces are found to have very fine grains but the contour and roughness of the surfaces remain the same due to the conformal coating as seen in Figure **3-4**. For the flat surface in Figure **3**-4B, there appears to be pinholes spread throughout the rocky surface which agrees with results in previous work. Additionally, the laser swaths appear to be the most prominent features for both convex and flat

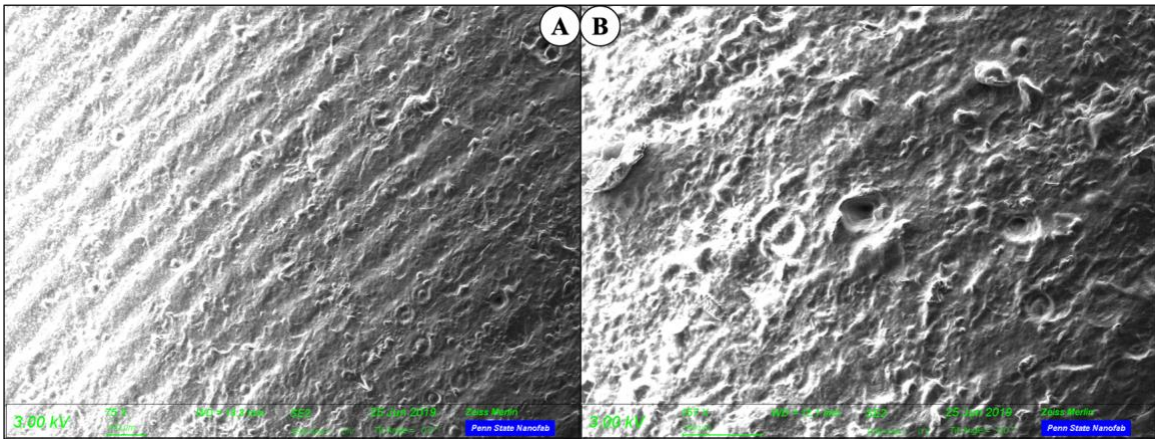

Figure **3-3**: 3D printed polymer dome surface.

surfaces. Particularly in Figure **3-4A**, there are lines along each concentric ring indicating a start and end position for the laser. It appears as though there is no way to avoid the trace of the laser. A closer look after PRC plating shows how fine the grains are for both convex and flat surfaces.

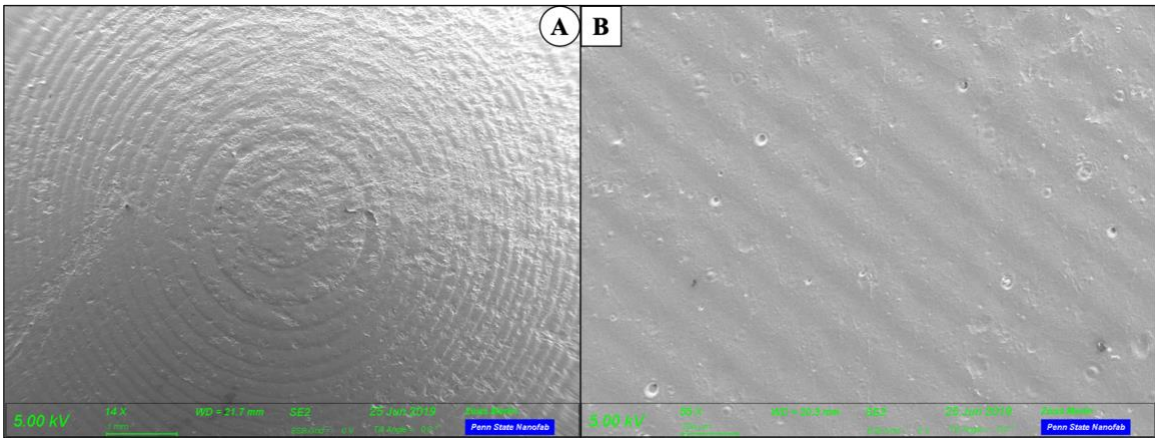

Figure **3-4**: After EBPVD, polymer (A) dome surface and (B) flat surface.

The two images in Figure **3-5** display similar grains after PRC plating which suggests the plating performance for convex and flat surfaces does not vary drastically. However, a radius of curvature equal to 15mm may not be sufficient to result in a drastic variation from a flat surface when considering a 25mm diameter.

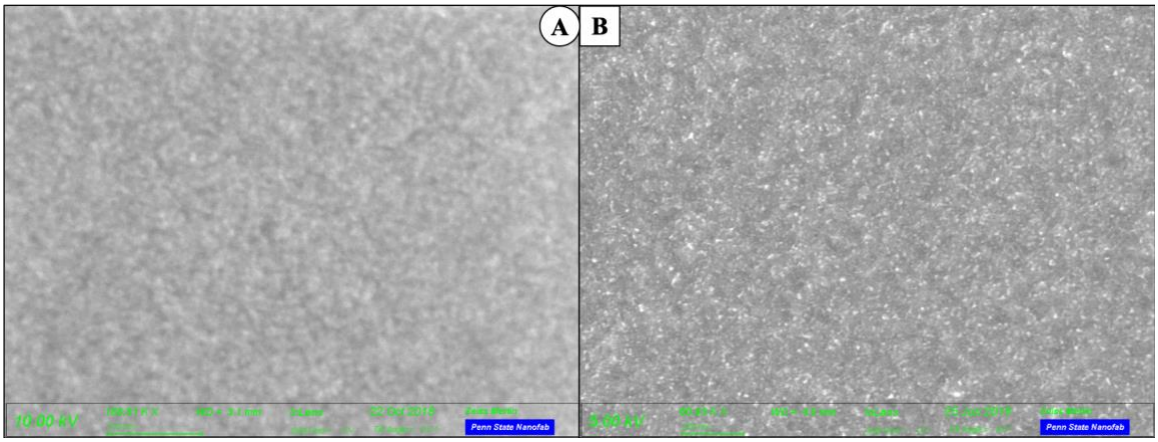

Figure **3-5**: After PRC plating, polymer (A) dome surface and (B) flat surface.

Imperfections

While additive manufacturing is capable of printing just about anything within the allowable build volume, there are some tradeoffs in the form of surface roughness and imperfections. Though, some of the following imperfections are not from printing. Instead, some of the procedures are likely the cause. For example, in Figure **3-6**, there are cracks in the coating which are likely due to thermal stress. Before restoring the chamber of the evaporator to

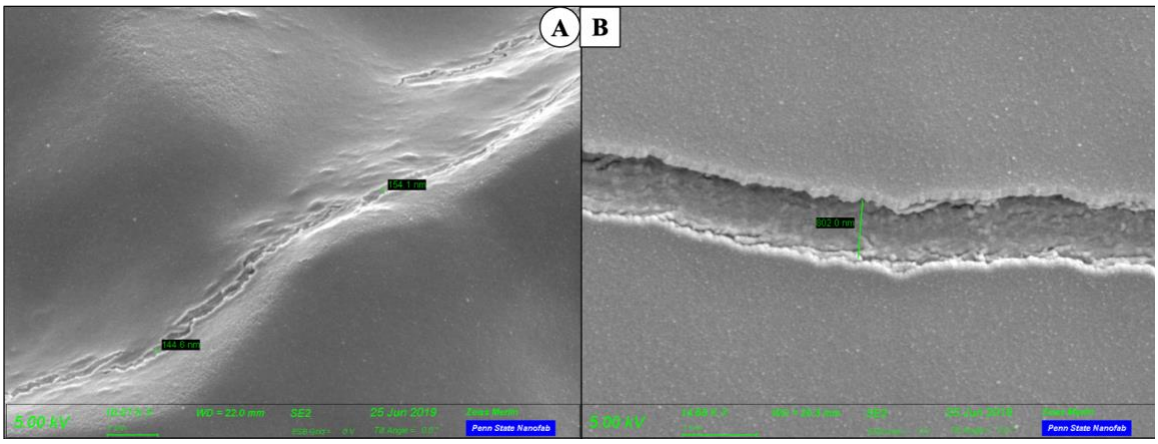

Figure **3-6**: After EBPVD, close-up of cracks on polymer (A) dome and (B) flat.

atmospheric pressure after EBPVD, an hour cooldown was enforced to prevent the cracks. However, this strategy does not appear to work. Either the cooldown time is not long enough or the cracks are from a different cause. Thermal stress is present during post-curing after dipping in the resin. The liquid resin is flash cured which could cause immediate cracks in the surface.

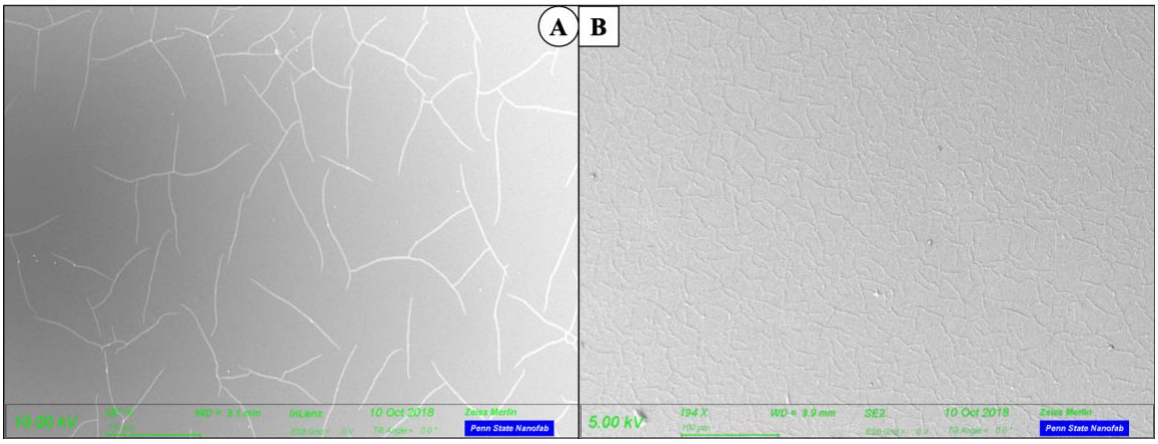

Figure **3-7**: After EBPVD, cracks on polymer (A) dome and (B) flat [1].

Figure **3-7** demonstrates how thermal stress behaves differently for convex and flat surfaces. Figure **3-7A** shows how the convex surface has long cracks. Whereas, Figure **3-7B** shows how the flat surface has many short, splintering cracks. The high vacuum, high temperature conditions

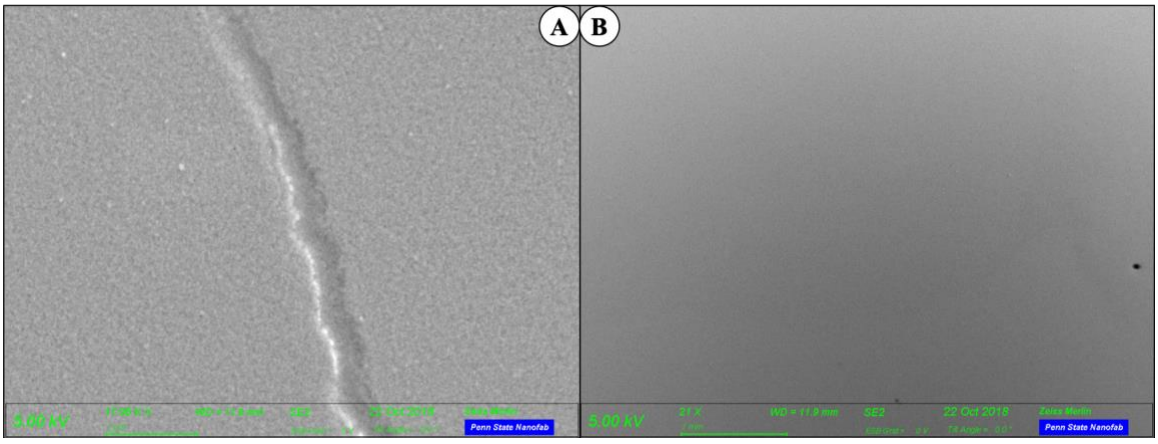

Figure **3-8**: After PRC plating, (A) close-up and (B) zoomed-out image of polymer dome [1].

seem to have less of an effect on convex surfaces than flat surfaces. Interestingly, PRC plating fills in the cracks to some degree in Figure **3-8A**. There are several small cracks that are filled completely, as though they never existed. However, large gaps and holes remain visible and are more difficult to handle. In Figure **3-9**, there are examples of holes on a 3D printed surface which

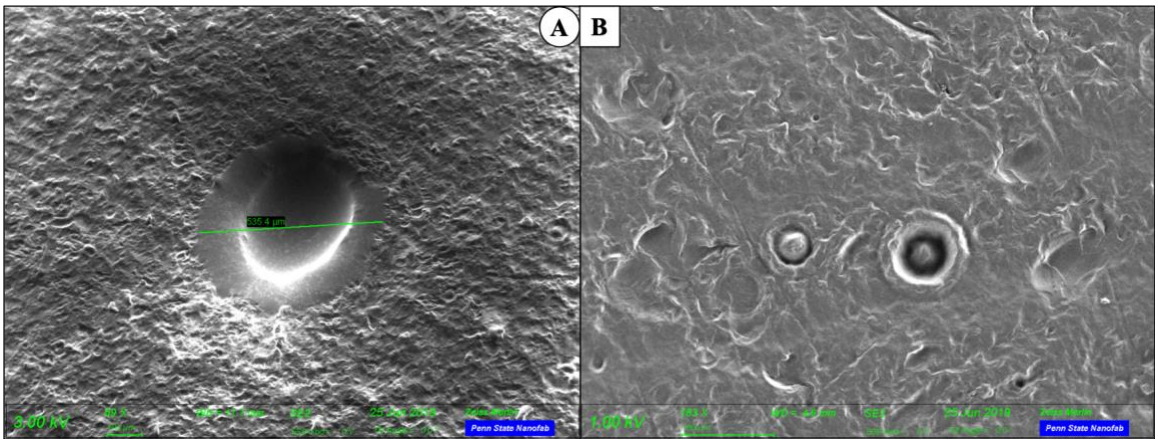

Figure **3-9**: After 3D printing, polymer (A) holes and (B) ring-like structures.

appear to be a result of the printing process in Figure **3-9B** or from carelessly handling the part in Figure **3-9A**. During the printing process, it is possible the resin tank becomes contaminated with partially cured resin. This could affect the print such that it blocks the laser from curing a portion

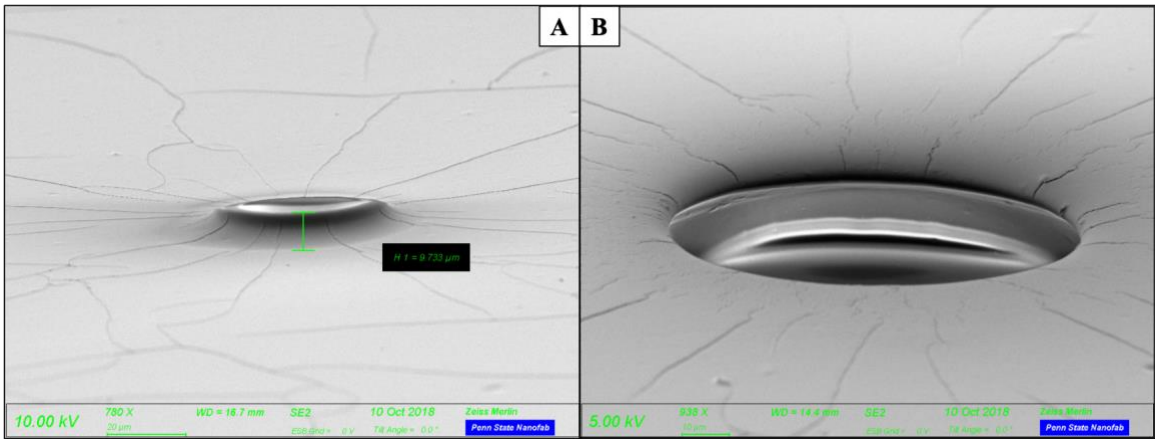

Figure **3-10**: After EBPVD, (A) volcanic-like and (B) sinkhole-like pinholes on polymer flat surface [1].

of the resin. Sometimes these particles become trapped and suspended within the part. Other times, they can end up on the surface. There are strategies to reduce the contaminants in the resin which should be considered if the application requires. Figure **3-10 and** Figure **3-11** show deep holes that are perfectly round. In previous work, outgassing and trapped air bubbles were discussed. However, Figure **3-9B** shows holes that are immediately after 3D printing. Therefore, it is possible the holes are from the printing process in addition to the causes discussed in previous work. In Figure **3-11**, PRC plating is capable of bridging the thin gap along the crack but fails to as it widens.

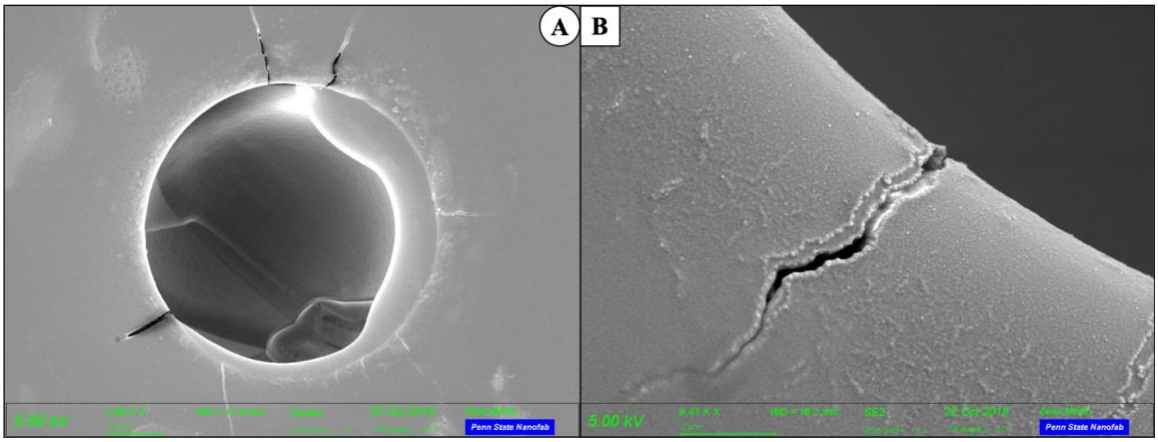

Figure **3-11**: After PRC plating, pinholes on polymer (A) dome and (B) flat surface.

Surface Roughness

The following data is obtained using optical profilometry and calculated in Mx software using a mask of fixed area and a form remove of a plane for flat surfaces or a cylinder for convex surfaces. No data fill or additional processing unless specified. Although several parameters are measured and provided, the primary focus of this report to understand how the surface roughness varies throughout procedures from surface to surface. Table **3-1** includes information on a flat

surface and convex surface. Each surface is measured after 3D printing, after EBPVD, and after PRC plating. The information for the flat surface is obtained from a mask in the middle region of the surface for best-case-scenario. For the convex surface, the information is obtained from the

Table **3-1**: Surface Characteristic Properties for Polymer Substrates

PROPERTIES	Flat Surface			Convex Surface		
	3D Printed	Post EBPVD	Post PRC Plated	3D Printed	Post EBPVD	Post PRC Plated
RMS (μm)	1.292	0.920	0.313	1.375	1.811	0.520
RA (μm)	1.037	0.757	0.254	1.150	1.504	0.423
PV (μm)	5.717	4.110	1.341	7.132	9.749	2.759
PEAK (μm)	2.383	1.933	0.515	3.449	4.938	1.084
MEAN (μm)	-0.005	0.014	0.000	-0.039	-0.037	0.027
VALLEY (μm)	-3.333	-2.176	-0.826	-3.683	-4.811	-1.675
LENGTH (μm)	978.26	979.183	979.031	991.732	984.951	715.622
RZ (μm)	3.834	2.339	0.770	4.315	6.831	1.975
RSK	-0.501	-0.114	-0.520	0.128	0.089	-0.036
RKU	2.649	2.328	2.749	2.294	2.563	2.568
SA (μm)	1.897	1.842	0.907	2.422	2.825	1.594
SQ (μm)	2.366	2.334	1.078	8.418	6.195	3.188
SZ (μm)	102.809	140.061	4.817	2012.696	1847.419	836.431

steepest region for worst-case-scenario. There is no OP data for the resin dipped substrates but it is discussed in previous work. SEM results show the resin dipped substrates have singicantly enhanced surface roughness. Figure **3-12** offers a visual of the surface roughness throughout the procedures. The first column is for the convex surface whereas the second column is for the flat surface. The first row is for after 3D printing, second is for after EBPVD, and third is for after PRC plating. The surface roughness is observed to remain the same for after 3D printing and after EBPVD; that is expected since EBPVD is a conformal coating procedure. After PRC plating, the surface roughness visually appears to improve, which agrees with the data in Table **3-1**.

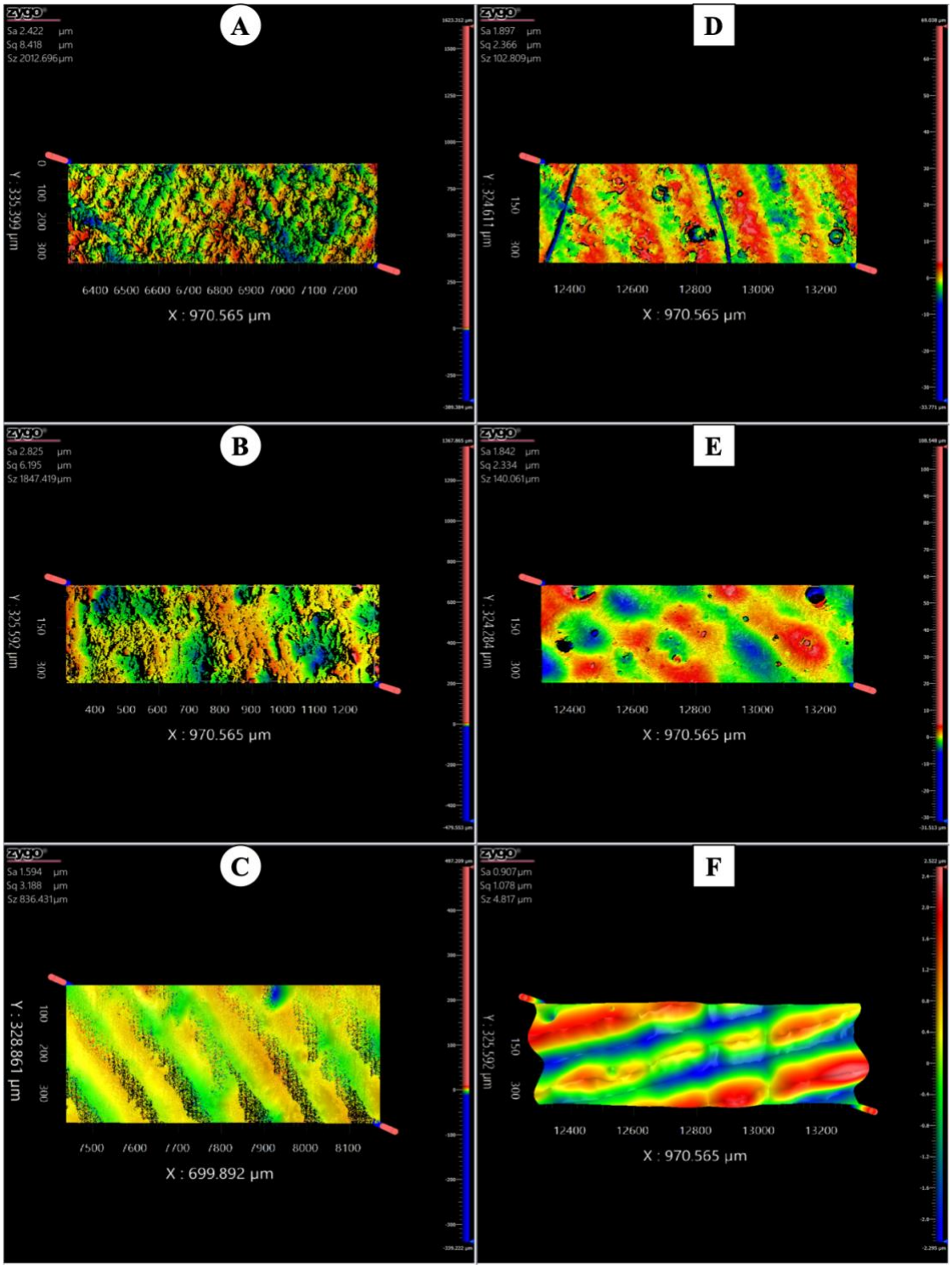

Figure **3-12**: OP data for (A) flat after 3D printing, (B) flat after EBPVD, (C) flat after PRC plating, (D) dome after 3D printing, (E) dome after EBPVD, (F) dome after PRC plating.

Chapter 4

Experimental Results and Observations for Metal Substrates

There are three metal substrates under evaluation for this report: a sample piece, a flat substrate, and a dome substrate.

Dimensional Characterization – Metal Substrate

Flatness, curvature, and diameter accuracy are determined using optical profilometry (OP) and scanning electron microscopy (SEM). Flatness is examined using the sample piece and the flat substrate whereas curvature is examined using the dome substrate. The diameter accuracy is tested for various-sized holes on the sample piece. OP measurements are executed across the diameter of each flat substrate and along a portion of the radius beginning at the apex for each dome substrate due to a maximum scan length. The scan width is about 335 micrometers.

Flatness

This section considers the sample piece and the flat substrate immediately after 3D printing and then after PRC plating. The following images and data are calculated using Mx software with a form remove of a plane. There is no data fill or additional processing. Figure **4-1** shows the maximum peak-to-valley throughout the middle of the flat substrate varies by about 40 μm along a 20000 μm horizontal distance. Along the outer edges, there are peaks that are about 100 μm tall. After PRC plating, the peak appears to be higher but the middle region has a lower maximum peak-to-valley.

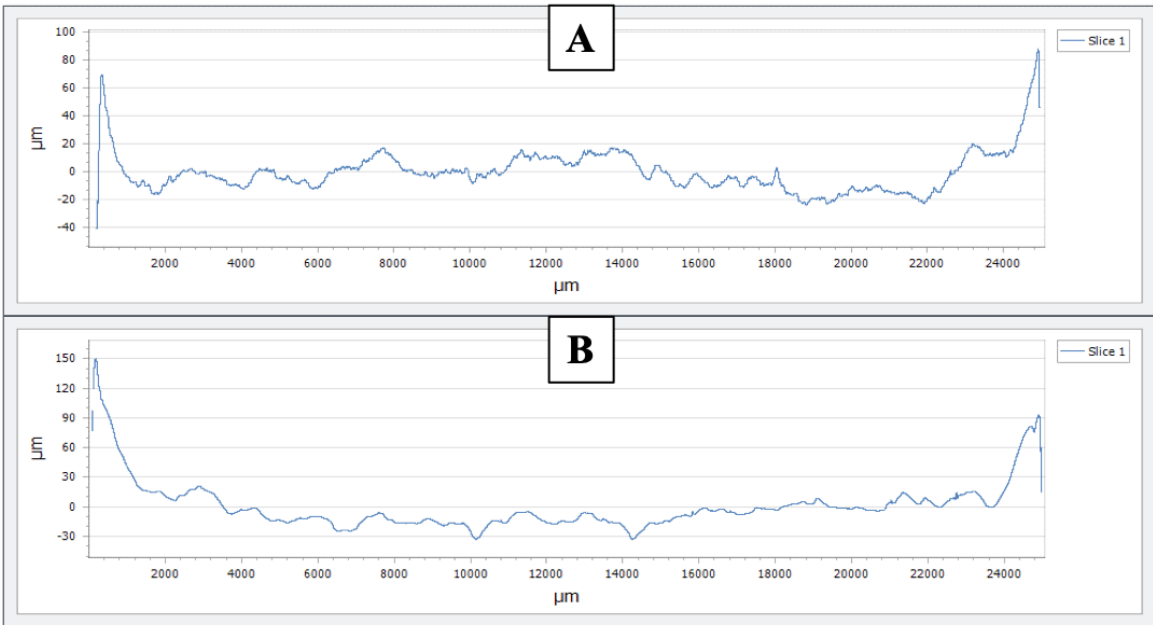

Figure **4-1**: Metal flatness data (A) after 3D printing and (B) after PRC plating.

The scan for flat substrates covers the entire diameter because the working distance is not exceeded. In Figure **4-2,** masks were applied to observe the 3D printed surface near the edge and the surface in the middle of the substrate. The surface near the edge in Figure **4-2A** shows the beginning of the steep peak observed in Figure **4-1A**. The laser swaths are also observed.

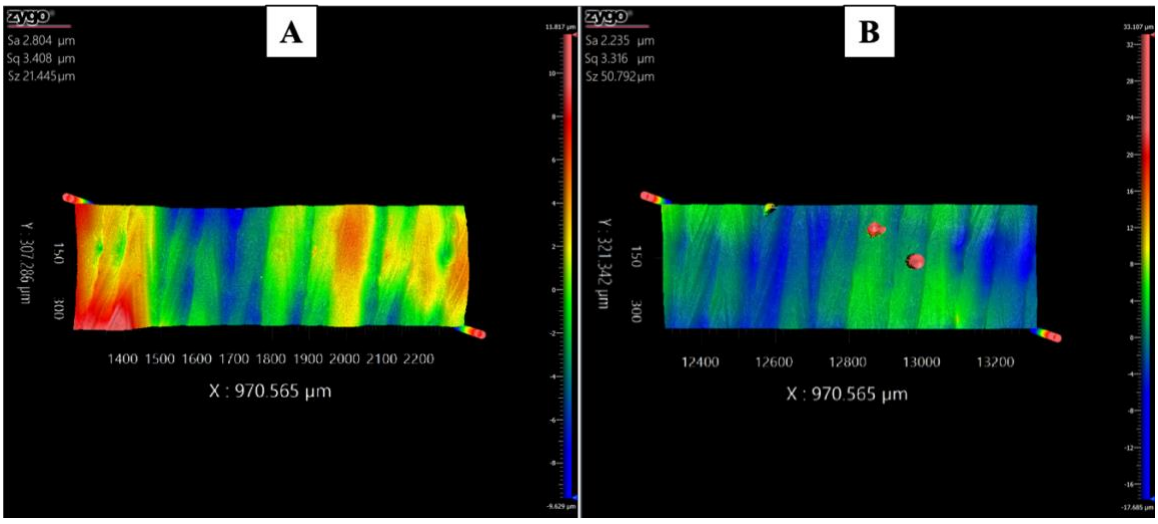

Figure **4-2**: After 3D printing, metal flat surface with mask (A) near edge and (B) in the center.

Figure **4-2B** is a portion of the scan in the center of the substrate which appears much smoother and more uniform than on the edge. Figure **4-3** is a similar comparison but it considers the flat substrate after PRC plating. While the center region contains less height variation than the edge, the uniformity does not appear to be improved by plating when compared to Figure **4-2B.**

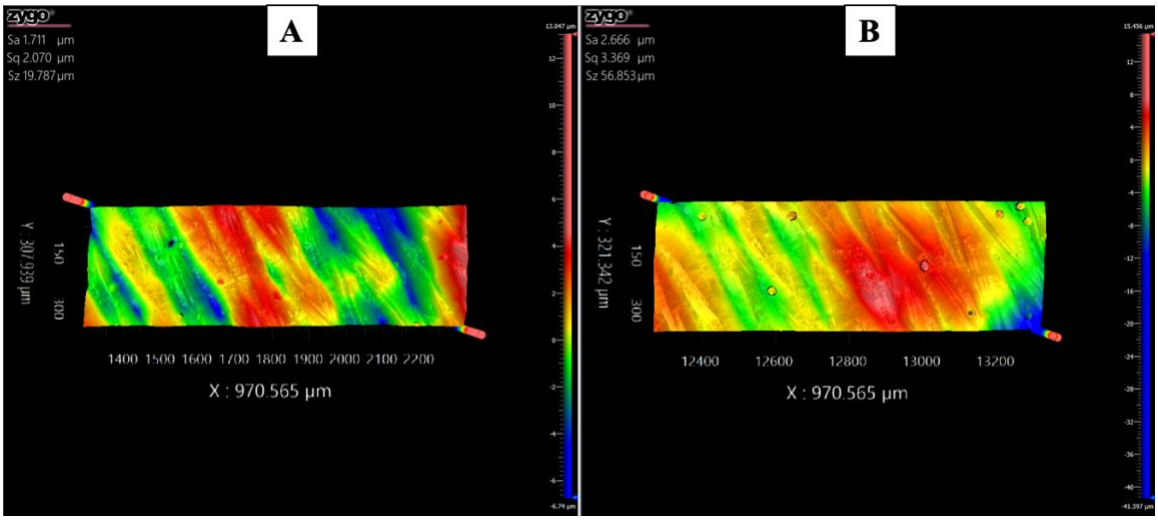

Figure **4-3**: After PRC plating, metal flat surface with mask (A) near edge and (B) in the center.

Curvature

This section focuses only on OP data collected from dome substrates. For this data, no form remove is applied. Each scan begins from the apex and extends radially until the scan length is maximized, limited by the working distance. Figure **4-4** displays substrate curvatures after 3D printing, after PRC plating, and bead-blasted after 3D printing. A green reference line is the curvature of the 3D CAD model. Based on the plot, the 3D dome and the 3D bead-blasted dome are observed to follow the reference curvature quite well. The bead-blasted dome appears to have a smoother surface than the rocky 3D printed dome. After PRC plating, the curvature veers away from the reference line and results in a greater radius of curvature, approaching a flatter surface.

Also, the curvature after PRC plating appears smoother than the curvature after 3D printing. These observations come with the assumption the graph is a true depiction of the substrate's curvatures. The vertical axis for each curve is shifted so the apex of all curves were intersecting at 0. No form remove was applied so any unintentional slant of the surface would play a role in this visualization.

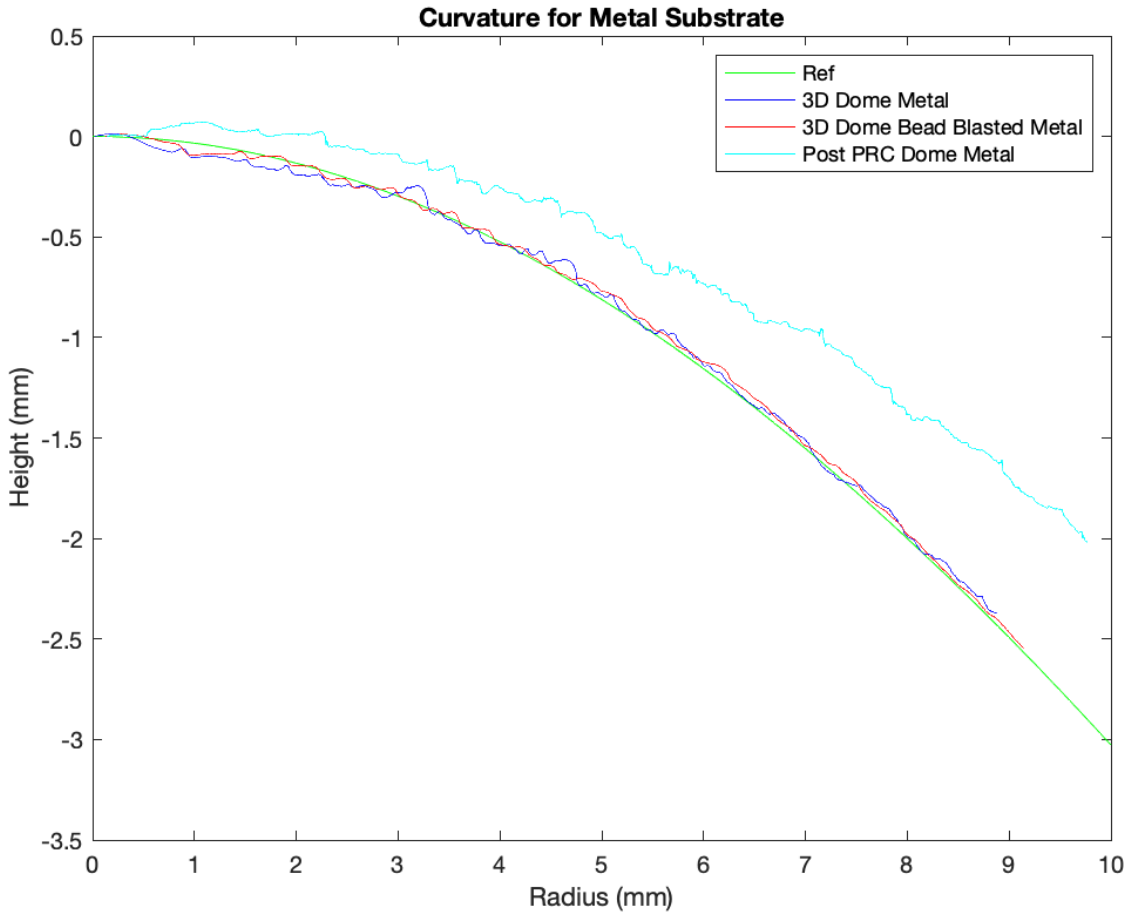

Figure **4-4**: Metal dome curvature plot.

Diameter Accuracy

Figure **4-5** includes SEM images of various-sized through-holes in the sample piece after PRC plating. A line on the image is a measurement of the diameter in micrometers taken on the SEM. Figure **4-5A** and Figure **4-5B** have diameters that are inconsistent whereas Figures **4-5C - E** have diameters that are consistent. It is worthy to note, the powder particles become trapped in these holes. If threading is required, the powder particles may cause some difficulty. It is likely the hole would need to be drilled after printing to clean it up.

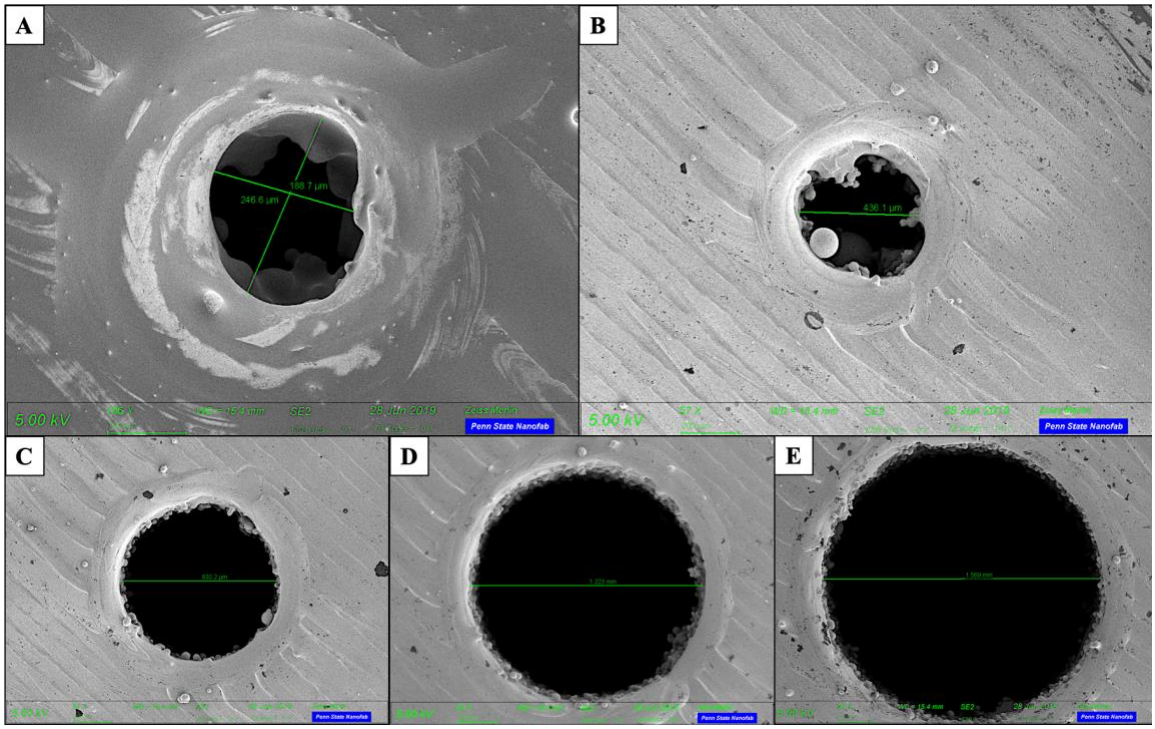

Figure **4-5**: After PRC plating, through-holes on sample piece: (A) 1/128in, (B) 1/64in, (C) 1/32in, (D) 3/64in, (E) 1/16in.

Table **4-1**: Diameter dimensions of through-holes for metal sample piece after PRC plating

PROPERTIES	Sample Piece				
	Post PRC Plating				
	1/128	1/64	1/32	3/64	1/16
3D Model Diameter (in)	0.0078125	0.015625	0.031250	0.046875	0.062500
Measured Diameter (in)	0.0085689	0.017169	0.032685	0.048150	0.061772

Surface Characterization – Metal Substrate

A combination of OP and SEM measurements are used to characterize the surface quality and surface roughness. All components are considered: the sample piece, the flat substrate, and the dome substrate. All procedures are considered: after 3D printing, after PRC plating, after bead-blasting, and after DC plating.

Surface Quality

Grain Size

The following provides before-and-after images for several inclined surfaces on the sample piece. In addition, before-and-after images of a dome are included with a comparison to a

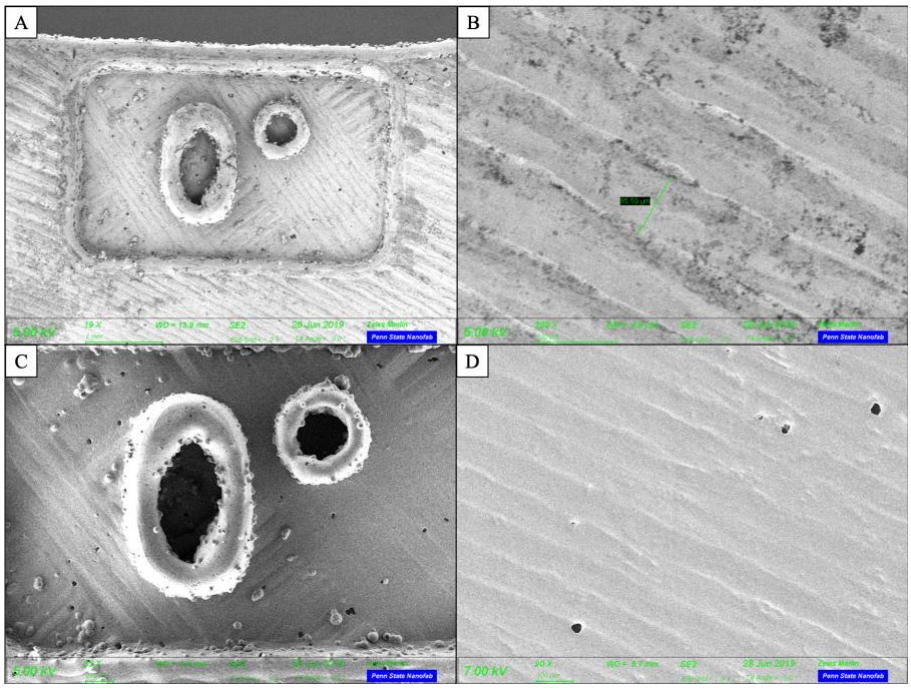

Figure **4-6**: Images of metal sample piece: 0-degree incline after 3D printing (A, B) and after PRC plating (C, D).

bead-blasted dome. Figure **4-6** shows a 0° incline. Not many powder particles are observed. The surface is relatively flat, comprising of only the laser swaths. The number and symbol written in metal are defined and readable. For all inclines, the number and symbol are printed with no incline. After plating, Figure **4-6C** and Figure **4-6D** show the surfaces are noticeably smoother.

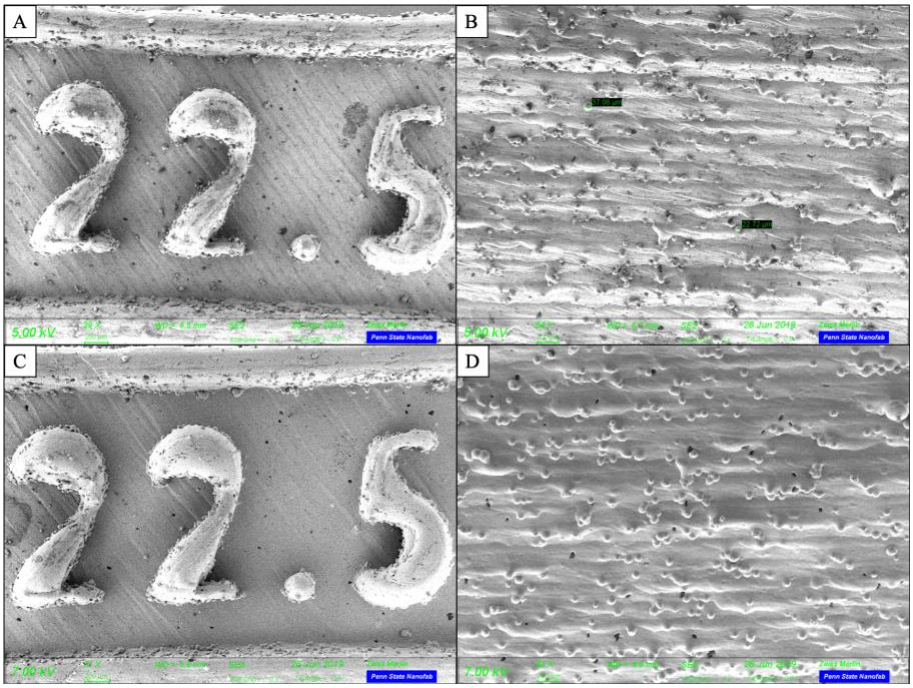

Figure **4-7**: Images of metal sample piece: 22.5-degree incline after 3D printing (A, B) and after PRC plating (C, D).

The laser swatch after plating appears to be faded. For inclines 22.5°, 45°, and 67.5°, the number of powder particles appear to increase as the incline increases. The powder particles appear to cause the surface to be much rougher than a flat surface. After plating, the powder particles do not fade as the laser swaths do. However, the surface of the powder particles become smoother. Figure **4-7D** shows how PRC plating is like a snowstorm of metal washed across the powder particles. They do not get completely buried but they do become smoother. Images of domes are

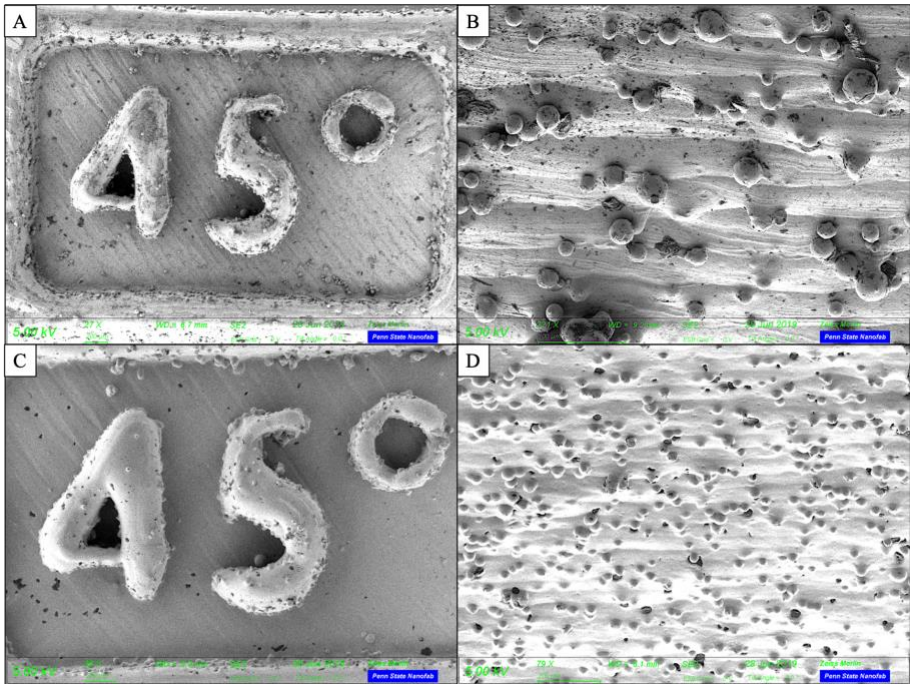

Figure **4-8**: Images of metal sample piece: 45-degree incline after 3D printing (A, B) and after PRC plating (C, D).

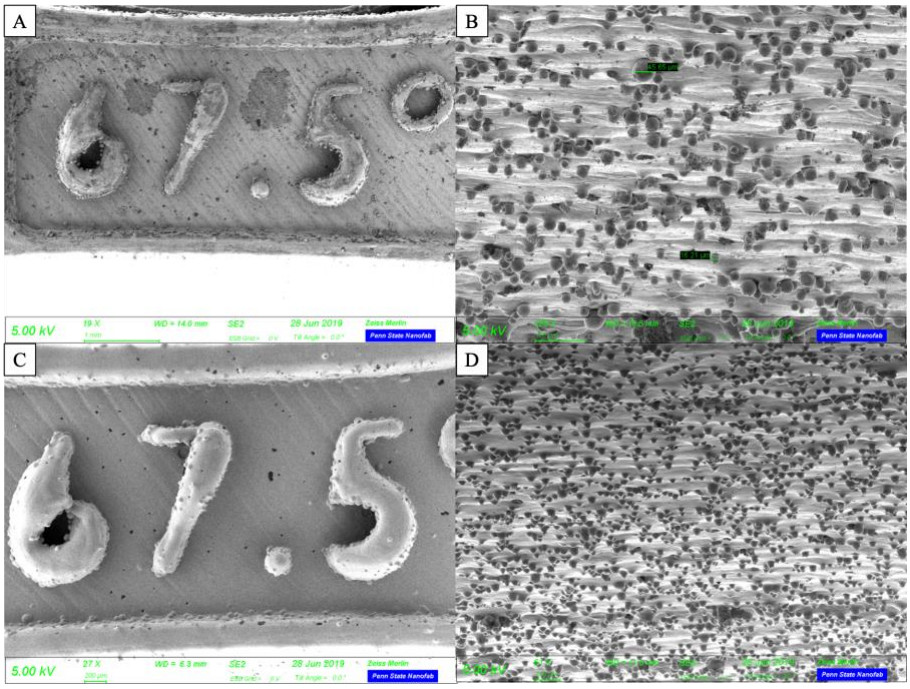

Figure **4-9**: Images of metal sample piece: 67.5-degree incline after 3D printing (A, B) and after PRC plating (C, D).

included in Figure **4-10** showing the impact of bead-blasting and DC plating. The surface in Figure **4-10C** is more uniform than Figure **4-10A** but neither is smooth. After DC plating, Figure **4-10B** seems much smoother than Figure **4-10D** but not as uniform. DC plating is a conformal coating process so the surface roughness should not improve much despite appearing like it does.

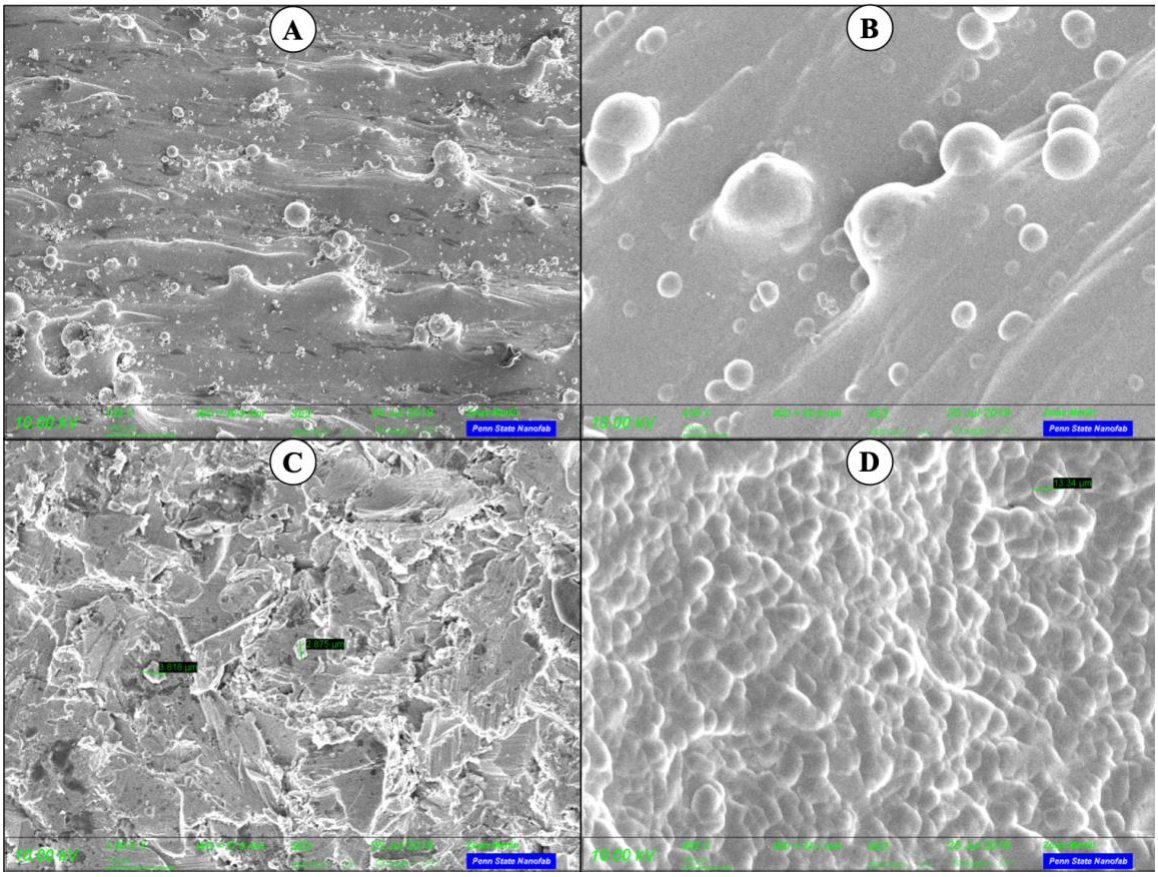

Figure **4-10**: Metal dome (A) after 3D printing, (B) after DC plating, (C) after 3D printing, then bead blasting, (D) after DC plating.

Imperfections

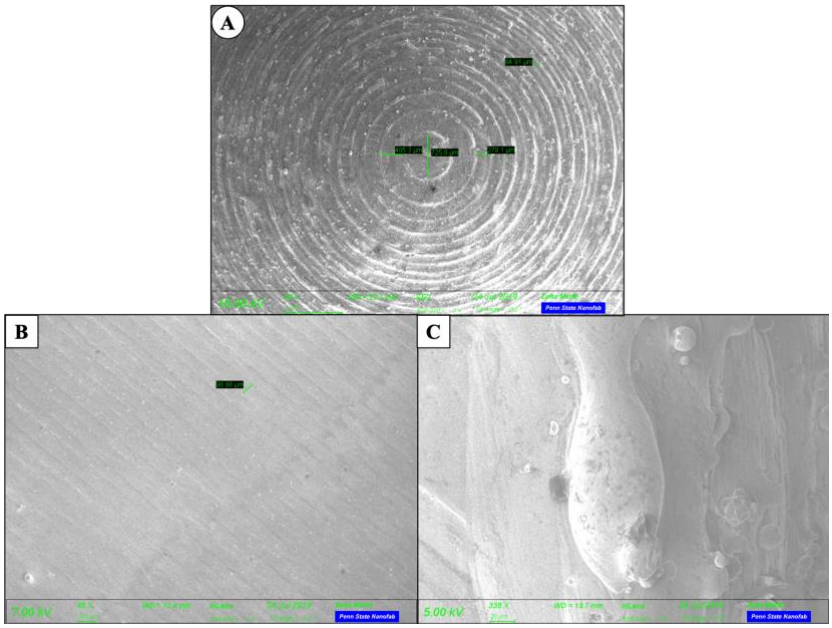

Figure **4-11**: Image of laser swath for (A) dome and (B, C) flat surface after 3D printing.

The laser swath accounts for the surface roughness on flat surfaces as seen in Figure **4-11B**. Therefore, it is difficult to produce parts with a smoother surface than the 90µm beam diameter. The outer edges of the substrate contain a gob of metal which causes the peak seen in Figure **4-1**. In addition, the laser swath is also a factor for domes as in Figure **4-11A** but the powder particles have greater effect. Figure **4-12** shows a close-up of the powder particles and

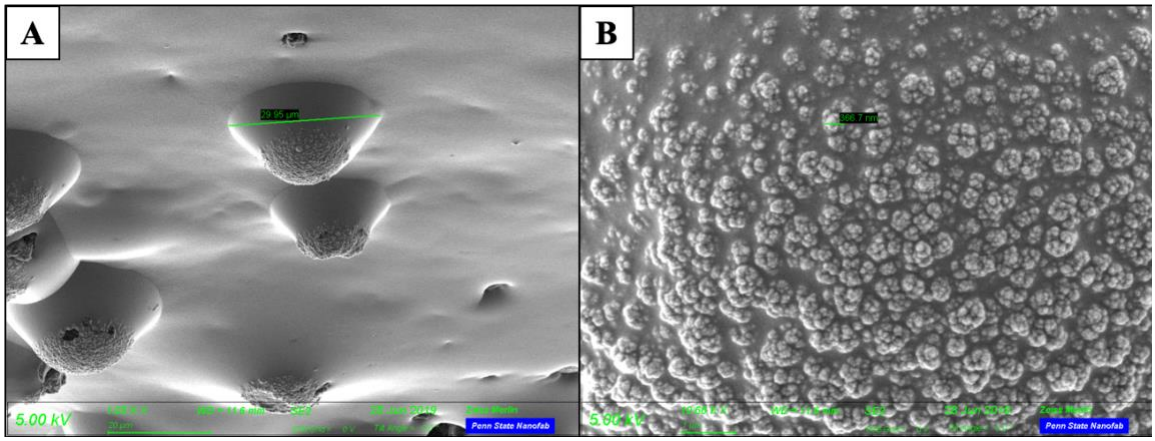

Figure **4-12**: Images of powder particles on sample piece at 67.5-degree incline after PRC plating.

how they play a role in the surface roughness. Moreover, a portion of the powder particle was not plated due to the steep inclination angle as demonstrated in Figure **4-13**.

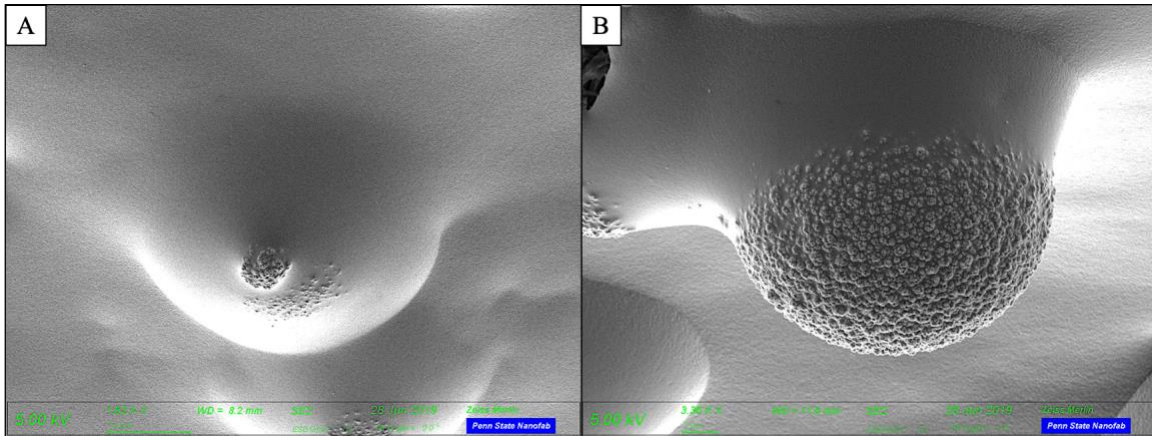

Figure **4-13**: Image of sample piece: after plating, (A) 45-degree and (B) 67.5-degree incline.

Surface Roughness

Table **4-2**: Surface Characteristic Properties for the Metal Sample Piece

PROPERTIES	Sample Piece			
	3D Printed			
ANGLE (deg)	67.5	45	22.5	0
RMS (μm)	13.003	8.285	12.528	1.311
RA (μm)	10.593	6.211	10.006	1.144
PV (μm)	63.071	46.67	58.826	5.509
PEAK (μm)	33.646	19.763	32.843	2.625
MEAN (μm)	2.764	0.527	-0.01	0.001
VALLEY (μm)	-29.425	-26.907	-25.983	-2.884
LENGTH (μm)	714.577	707.22	705.693	707.65
RZ (μm)	49.872	23.591	22.213	2.52
RSK	0.638	-0.283	-0.031	-0.265
RKU	2.582	3.831	2.962	1.88
SA (μm)	17.978	9.774	11.175	1.416
SQ (μm)	22.686	13.411	14.276	1.747
SZ (μm)	2273.828	1775.489	652.342	14.49

Table **4-2** shows the surface roughness for various inclination angles of the sample piece after 3D printing. Results agree with the SEM images above such that the surface is smoother for the 0° inclination and rougher for the 67.5° inclination. Data for the surfaces after PRC plating are omitted because there are not enough collected points to be reliable as seen in Figure **4-14**.

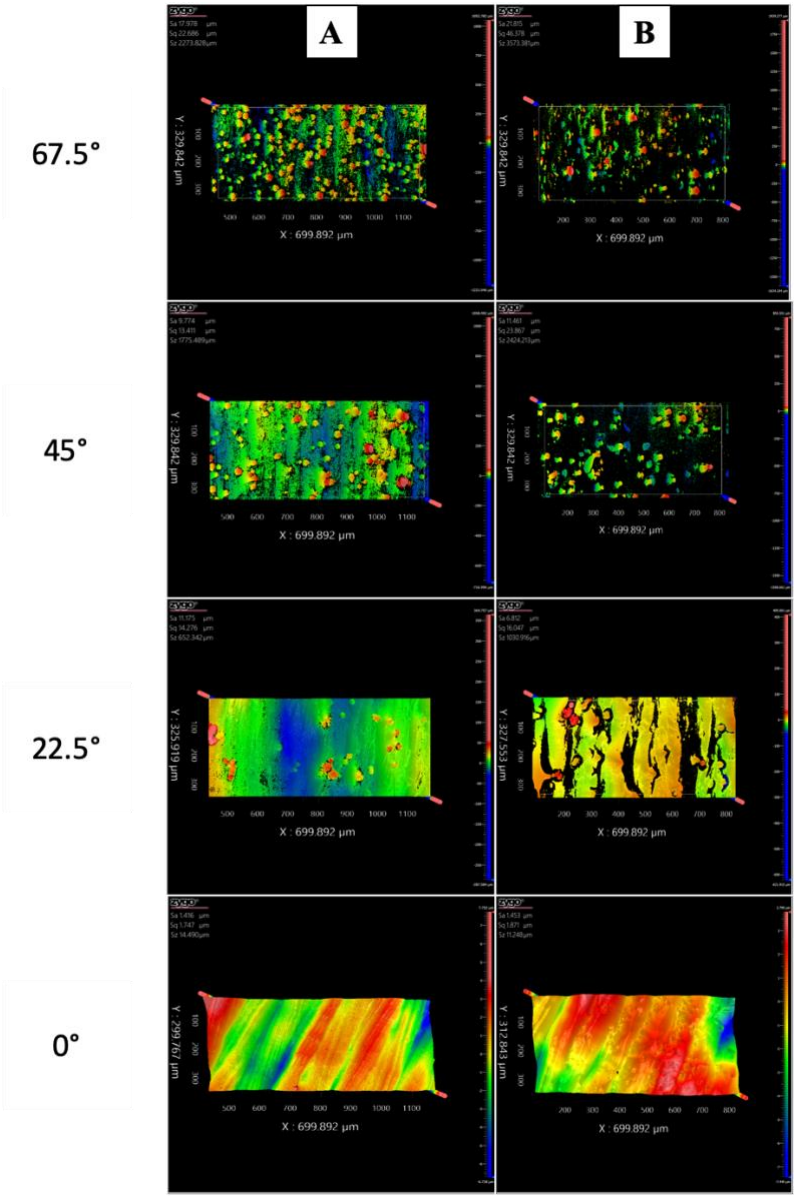

Figure **4-14**: Metal sample piece. flat surfaces for an incline of 67.5-degrees, 45-degrees, 22.5-degrees, and 0-degrees A) after 3d printing and B) after PRC plating.

Table **4-3** comprises of data for flat and convex surfaces after 3D printing, after PRC plating, and after bead-blasting. Data is extracted from flat surfaces using a mask in the central region of the substrate to get a best-case-scenario. A form remove of a plane is applied. For domes, the mask is applied as far radially from the apex as possible to get a worse-case-scenario. A form remove of a cylinder is applied. The surface roughness does not appear to change very much after PRC plating which is likely due to how large the powder particles are in comparison to the plating particles. It is apparent the flat surface is not nearly as rough as the convex surface. In addition, the bead-blasted surface is smoother than the 3D printed counterpart. The maximum peak-to-valley for convex surfaces is greater the 30 μm width of the powder particles which suggests there may be additional factors than the powder particles. When considering the maximum peak-to-valley for the bead-blasted dome, it is interesting how the 15 μm value is 30 μm less than the 3D printed dome. After all, bead-blasting would detach the powder particles and these results may confirm it. Figure **4-15** provides a visual aid for the surface roughness values.

Table **4-3**: Surface Characteristic Properties for Metal Flat and Convex Substrates

PROPERTIES	Flat Surface		Convex Surface		
	3D Printed	Post PRC	3D Printed	Post PRC	Bead Blasted
RMS (μm)	2.146	2.818	15.399	16.855	6.862
RA (μm)	1.779	2.417	13.144	13.839	5.494
PV (μm)	8.967	10.795	73.704	85.064	28.638
PEAK (μm)	5.352	4.583	46.049	42.732	15.007
MEAN (μm)	-0.011	0.003	0.012	-1.692	0.023
VALLEY (μm)	-3.615	-6.212	-27.655	-42.332	-13.631
LENGTH (μm)	981.065	967.564	991.658	984.168	982.946
RZ (μm)	4.872	4.146	36.023	50.158	16.148
RSK	0.256	-0.074	0.015	-0.214	-0.014
RKU	2.217	2.178	2.413	2.695	2.445
SA (μm)	2.235	2.666	14.125	16.374	6.643
SQ (μm)	3.316	3.369	17.251	23.292	8.348
SZ (μm)	50.792	56.853	612.847	1612.75	615.057

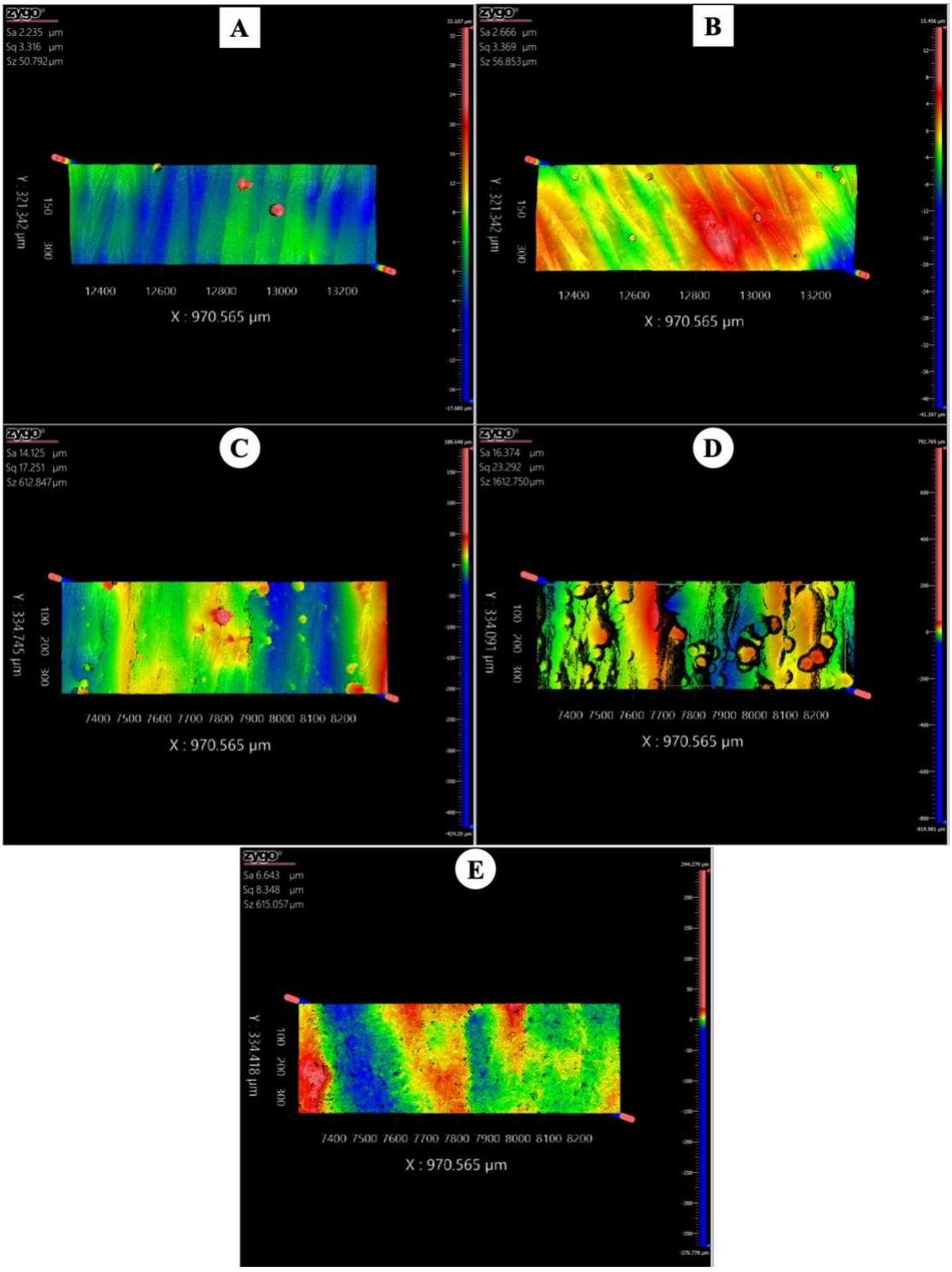

Figure **4-15**: Flat surface (A) after 3D printing and (B) after PRC plating; dome surface (C) after 3D printing (D) after PRC plating and (E) after 3D printing, then bead blasting.

Chapter 5

Conclusion

Discussion

All data in this report is obtained using optical profilometry and scanning electron microscopy. Images provided have several details that play a significant role in how the data is handled which will determine the reliability of the data.

Results for the polymers are promising for mirror development at infrared wavelengths. Data collected in this report suggest a submicron surface roughness can be achieved by 3D printing, metallizing via EBPVD, and PRC plating. The surface roughness can be significantly improved by a smaller laser beam diameter for printing or by dipping in resin after printing as demonstrated in previous work. Avoiding the high vacuum, high temperature environment of vapor deposition could also be a strategy to mitigate cracks and pinholes. Though, this report demonstrates polymer substrates can withstand such environment. With improvements, polymers will be capable of being additively manufactured for optical designs at visible wavelengths.

Results for the metals suggest further development needs to be made for mirror fabrication using additive manufacturing. Data collected returns a surface roughness in the micron range. It is believed the roughness is primarily due to 30μm powder particles but the 90μm laser swath is also shown to play a role. Bead-blasting is demonstrated to produce a smoother surface and appears to produce a more uniform surface. Some advantages of metal 3D printing are the parts come out to be very accurate and the surface can be directly electroplated.

Further Development

Since polymers can withstand high vacuum, high temperature during vapor deposition, testing how the shape deforms during the process could provide interesting results for space–related applications. For metal printers, it would be advantageous to have a post-print high power scan over the final surface, melting away any stray powder particles. In addition, an automated bead-blasting mechanism could be beneficial for ensuring uniformity across the surface without causing damage.

Appendix

Appendix A - Nomenclature

μm - microns, micrometers

3D - three-dimensional

ABS - acrylonitrile butadiene styrene

Au – gold

CAD – computer aided design

DC – direct current

EBPVD - electron-beam physical vapor deposition

EP - electroplating

FDM - fused deposition modeling

IR – infrared

Ni - nickel

OP - optical profilometry

PRC - pulse-reverse-current

SEM - scanning electron microscopy

SLA - stereolithography

SLS - selective laser sintering

Appendix B - Equipment

Electroplating Wet Bench in PSU NanoFab

EOS M280 Printer

Form2 Printer

M4L Plasma Generator in PSU NanoFab

Semicore Evaporator in PSU NanoFab

Scanning Electron Microscope in PSU NanoFab

ZEISS Smartzoom 5 – Automated Digital Microscope

ZYGO Optical Profilometer

BIBLIOGRAPHY

[1] J. C. Davidson, A. D. O'Neill, *et al*, "Surface methodology for 3D printed multispectral systems," in 2019. DOI: 10.1117/12.2519548.

[2] S. Jasveer and X. Jianbin, "Comparison of different types of 3D printing technologies," International Journal of Scientific and Research Publications (IJSRP), vol. 8, no. 4, pp. 1–9, Apr. 2018.

[3] H. Bikas, P. Stavropoulos, and G. Chryssolouris, "Additive manufacturing methods and modelling approaches: a critical review," International Journal of Advanced Manufacturing Technology, vol. 83, no. 1–4, pp. 389–405, Jul. 2015.

[4] W. E. Frazier, "Metal Additive Manufacturing: A Review," Journal of Materials Engineering and Performance, vol. 23, (6), pp. 1917-1928, 2014.